

Integration of Research for an Exhaust Thermoelectric Generator and the Outer Flow Field of a Car

T. JIANG,¹ C.Q. SU,^{1,2,3} Y.D. DENG,¹ and Y.P. WANG¹

1.—Hubei Key Laboratory of Advanced Technology for Automotive Parts, Wuhan University of Technology, Wuhan 430070, China. 2.—Hubei Collaborative Innovation Center for Automotive Components Technology, Wuhan University of Technology, Wuhan 430070, China. 3.—e-mail: suchuqi@whut.edu.cn

The exhaust thermoelectric generator (TEG) can generate electric power from a car engine's waste heat. It is important to maintain a sufficient temperature difference across the thermoelectric modules. The radiator is connected to the cooling units of the thermoelectric modules and used to take away the heat from the TEG system. This paper focuses on the research for the integration of a TEG radiator and the flow field of the car chassis, aiming to cool the radiator by the high speed flow around the chassis. What is more, the TEG radiator is designed as a spoiler to optimize the flow field around the car chassis and even reduce the aerodynamic drag. Concentrating on the flow pressure of the radiator and the aerodynamic drag force, a sedan model with eight different schemes of radiator configurations are studied by computational fluid dynamics simulation. Finally, the simulation results indicate that a reasonable radiator configuration can not only generate high flow pressure to improve the cooling performance, which provides a better support for the TEG system, but also acts as a spoiler to reduce the aerodynamic drag force.

Key words: Exhaust, thermoelectric generator, radiator, flow field, spoiler

INTRODUCTION

For the internal combustion engine vehicle, a thermoelectric generator (TEG) is a potential device to recover exhaust heat. The TEG tests on SUV and truck illustrated that it has the advantage of no moving parts and direct heat to electrical conversion,¹ but the efficiency is insufficient for practical use.² To improve the efficiency of the TEG on cars, the main challenges are the performance of the thermoelectric modules, the design of the heat exchangers and the cold source and maintaining sufficient temperature difference across the thermoelectric modules under different engine conditions.³

The basic research of TEG is the type, connection and configuration of the thermoelectric modules, such as the transverse and circular configuration.⁴ A temperature-controlled TEG during the driving

cycle is used to maintain the efficiency of the modules.⁵ The heat exchanger in an exhaust duct is an important part in TEG, and the optimization of its internal structures and thicknesses can improve the interface temperature and thermal uniformity.⁶ The cold source in TEG is quite important as it contains several cooling units, which absorb the heat in thermoelectric modules, and most of the cold source research focuses on the configuration and inner structure of the cooling units to increase cooling performance.⁷

However, the cooling units need the cooling device to work continuously. There are two technical routes for a cooling device. The first one is that the cooling units are connected to the engine cooling system as shown in Fig. 1. There is a long distance between TEG and engine cooling system, entailing additional water pump power, which may affect the heat balance of the engine.⁸ Figure 2 illustrates the other technical route in which the cooling units are connected to an independent radiator with a fan,

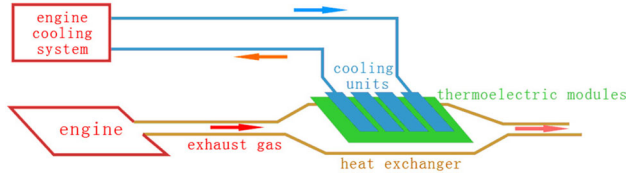


Fig. 1. Cooling by engine cooling system.

which needs more power to work continuously to take away the heat.

This paper proposes a technical route for a cooling device, in which the high speed underbody flow is used to take away the heat of the radiator and the cooling units, as shown in Fig. 3. What is more, a rational position and design of the radiator can increase the wind pressure and flow speed on the radiator surface, thus taking away more heat of the radiator.

The TEG radiator installed on a car chassis can also act as a spoiler to reduce aerodynamic drag force of the car. For example, as shown in Fig. 4, several spoilers installed near the exhaust duct in an Audi A6 are used to optimize the flow field around the chassis,⁹ without considering the cooling purpose.

In a word, this paper proposes a practical method to cool the TEG radiator. Afterwards, the wind pressure on the radiator surface and the aerodynamic drag force are compared between eight different schemes of radiator configurations by the Computer Fluid Dynamics (CFD) method.

The rest of the sections of this paper are organized in the following order: The CFD preparation and simulation result are introduced in Sect. 2. Section 3 illustrates the radiator schemes research. Finally, Sect. 4 shows the conclusions.

GEOMETRY AND SIMULATION

Geometric Model

Though cars are different in size and structure, the integration research method of TEG and the flow field is nearly the same. A sedan model with the length of 5018 mm, width 1890 mm, height 1490 mm and wheelbase 2950 mm is created for the simulation. As the key simulation area is near the exhaust duct, it is necessary to simplify the sedan model, which is shown in Fig. 5.

The heat exchanger in the TEG device is installed on the exhaust duct, in front of the muffler. The hot and cold sides of the thermoelectric modules are in contact with the heat exchanger and cooling units, respectively. It is noted that the cooling units contain several groups of water tanks, which are fixed together by clamping tools. The heat exchanger, thermoelectric modules and cooling units are considered as an integrated geometry in simulation, and the remaining part of the TEG is the radiator consisting of thin metal plates with U-shaped pipes

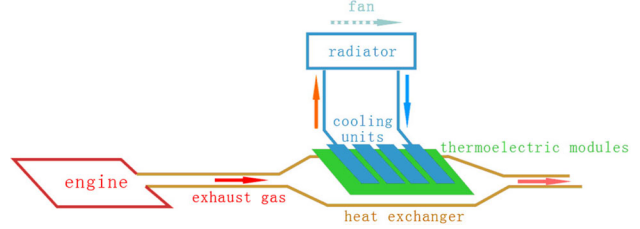


Fig. 2. Cooling by static radiator and fan.

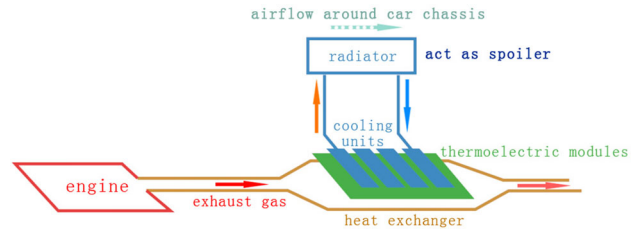


Fig. 3. Cooling by radiator and airflow in car chassis.

inside. As it shows in Fig. 6, the radiator is connected with the cooling units by flexible pipes.

As the attention is paid to the TEG radiator configuration around the chassis, the details and gaps in heat exchanger and radiator are eliminated for the purpose of improving mesh quality and saving computational resources in CFD simulation. Therefore, the indispensable TEG device, exhaust duct, fuel tank, spare tire slot and muffler are in detail created for the sedan model, as shown in Fig. 7.

Computational Model

In this simulation the flow is considered to be incompressible and steady. There are several types of Reynolds Averaged Navier–Stokes Equations (RANS), which are used to predict massively separated flows. One of the RANS is a realizable $k - \varepsilon$ turbulence model, which has the highest accuracy according to the experimental results.¹⁰ Therefore, a realizable $k - \varepsilon$ turbulence model is employed in this paper, and its governing equations are written as follows,¹¹

$$\frac{\partial(\rho k)}{\partial t} + \frac{\partial}{\partial x_i}(\rho k u_i) = \frac{\partial}{\partial x_j} \left[\left(\mu + \frac{\mu_t}{\sigma_k} \right) \frac{\partial k}{\partial x_j} \right] + G_k + G_b - \rho \varepsilon - Y_M, \quad (1)$$

$$\frac{\partial}{\partial t}(\rho \varepsilon) + \frac{\partial}{\partial x_i}(\rho \varepsilon u_i) = \frac{\partial}{\partial x_i} \left[\left(\mu + \frac{\mu_t}{\sigma_\varepsilon} \right) \frac{\partial \varepsilon}{\partial x_i} \right] + \rho C_1 S \varepsilon - \rho C_2 \frac{\varepsilon^2}{k + \sqrt{v \varepsilon}} + C_{1\varepsilon} \frac{\varepsilon}{k} C_{3\varepsilon} G_b, \quad (2)$$

where x_i is the position vector and ρ is the fluid density. u_i is the velocity vector and k is the turbulent kinetic energy and ε is the turbulence dissipation. G_k and G_b represent the generation of

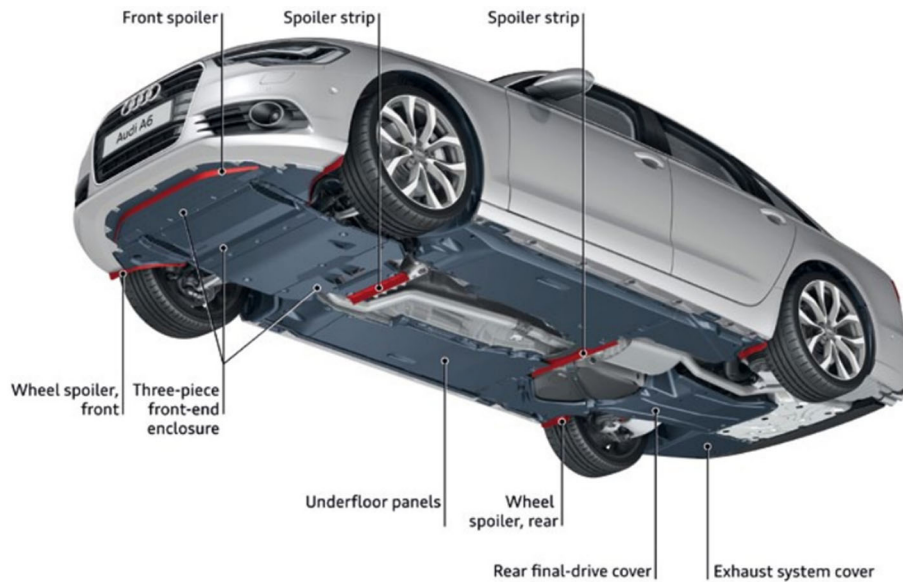


Fig. 4. Spoilers on car chassis near exhaust duct.

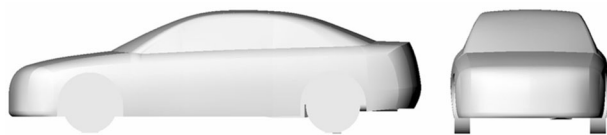


Fig. 5. CAD model of the car.

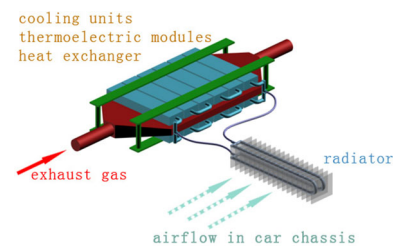


Fig. 6. The heat exchanger and the radiator.

the turbulence kinetic energy due to the mean velocity gradients and buoyancy, respectively. Y_m is the contribution of the fluctuating dilatation in compressible turbulence to the overall dissipation rate. μ is the viscosity and μ_t is the turbulent viscosity. $C_2 = 1.9$, $C_{1\varepsilon} = 1.44$. $\sigma_\varepsilon = 1.2$ and $\sigma_k = 1.0$ are the turbulent Prandtl number for k and ε , $C_1 = \max [0.43, \frac{\eta}{\eta+5}]$, $\eta = S \frac{k}{\varepsilon}$, $S = \sqrt{2S_{ij}S_{ij}}$, S_{ij} is the rate-of-strain tensor.

Mesh Generation

A computational domain, which is ten times the length, four times the width and height of the car is created around the car. The domain length behind the car is six times in magnitude to capture the essential flow features,¹² as shown in Fig. 8.

The meshes are generated by the ANSYS ICEM, which is a commercial pre-processing program in CFD analysis. The space near the exhaust duct is meshed with fine elements. After generating the volume mesh, the boundary layer effect is evaluated by 3.64 mm constructed boundary prism layers from the car surface. The number of unstructured tetrahedral hybrid elements is 5.21 million, as shown in Fig. 9.

Boundary Conditions

The boundary conditions applied by the mesh model by ANSYS FLUENT are listed in Table I.

RESULTS

After mesh generation without TEG radiator, the computation results are as follows:

The aerodynamic drag coefficient of the car is 0.3074. The projection area of the car in the flow direction is 2.223 m², and the drag force is 376.7 N, when the speed is 30 m/s. The static pressure distribution around the chassis is plotted in Fig. 10, which illustrates the exhaust duct, fuel tank, heat exchanger, rear wheel, muffler and rear end experiencing high pressure, and the flow gets stagnated at the above mentioned places. The flow remains attached to the middle and side of the chassis with low pressure. It is necessary to analyze and improve the aerodynamics performance when installing a TEG on the car.

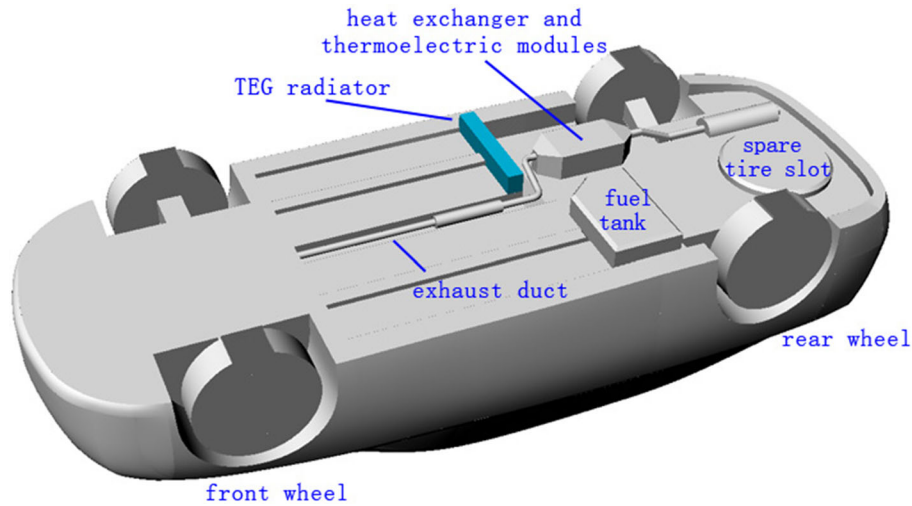


Fig. 7. Chassis CAD model for CFD simulation.

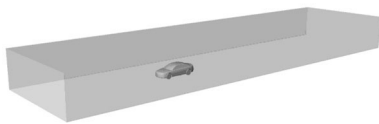


Fig. 8. Computational domain for car model.

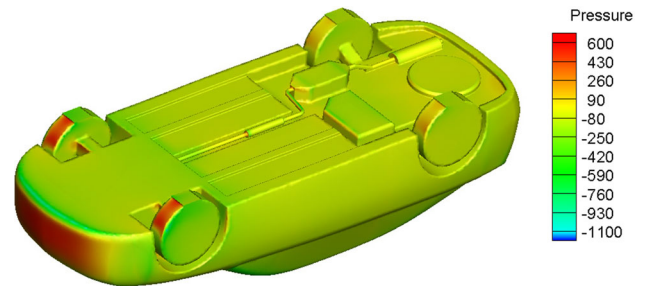


Fig. 10. Static pressure distribution.

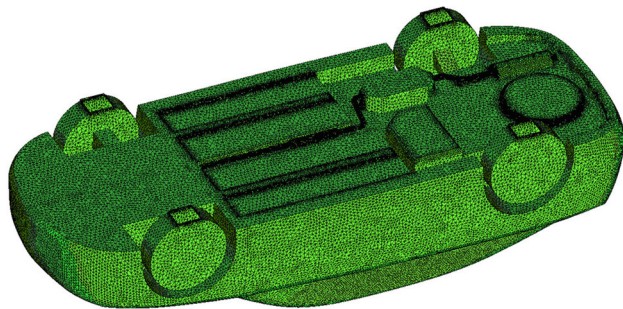


Fig. 9. Mesh generation in the chassis.

SCHEMES RESEARCH

Schemes Configurations

The radiator has a shape that may be rectangle or ladder-shaped and should meet the standards of the spoiler and is constrained by ground clearance of the car and chassis structure. Eight schemes are designed and simulated with the same boundary conditions.

Scheme 1: Higher radiator in front of the fuel tank. Static pressure distribution is shown in

Table I. Boundary conditions

Boundary	Boundary conditions and value
Inlet	Constant velocity = 30 m/s, Turbulent intensity = 0.5%
Outlet	Pressure outlet, Gauge Pressure = 0 pa Turbulent intensity = 5%
Ground	Moving wall = 30 m/s, no slip
Domain top and side wall	Stationary wall, no slip
Car	Stationary wall, no slip

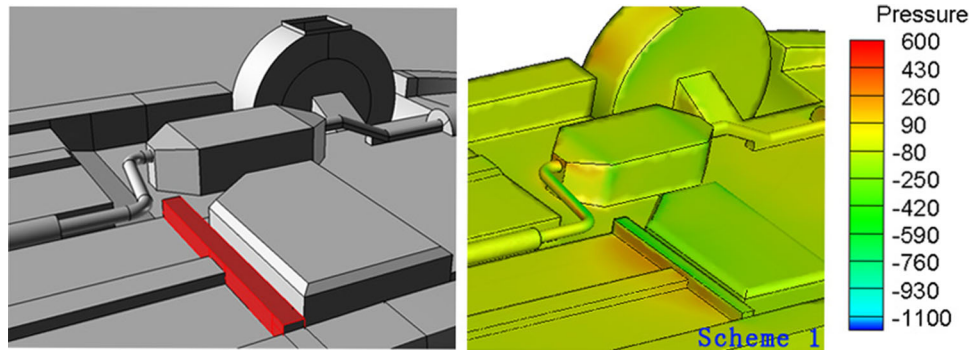


Fig. 11. Model and pressure distribution in Scheme 1.

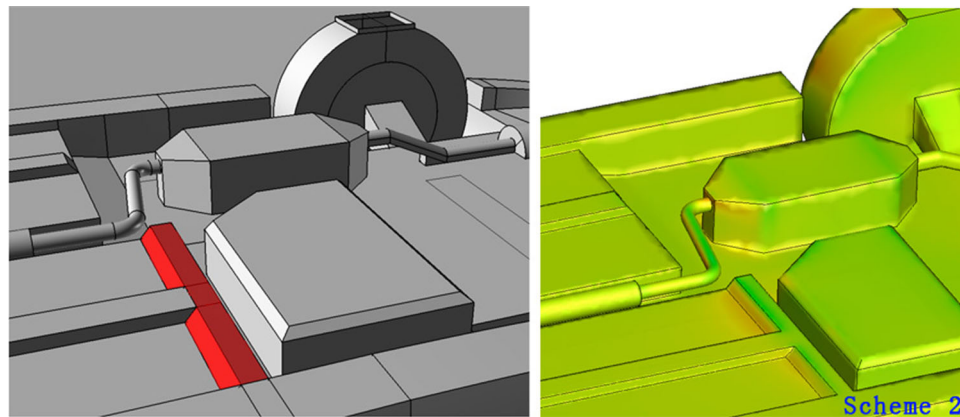


Fig. 12. Model and pressure distribution in Scheme 2.

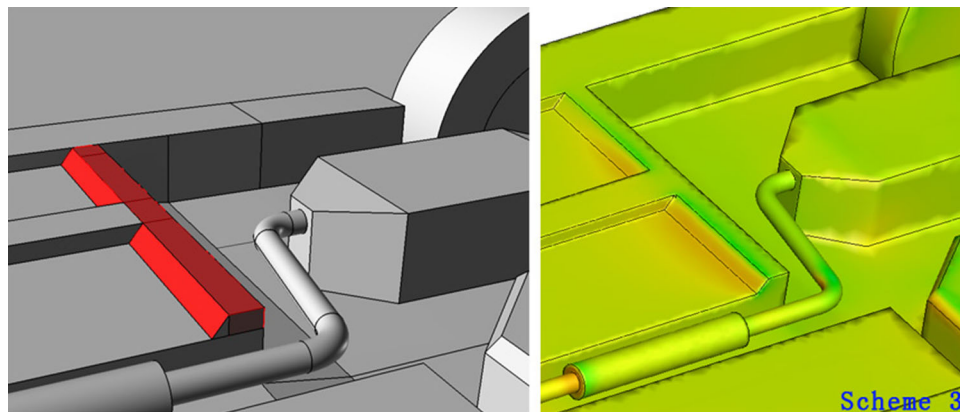


Fig. 13. Model and pressure distribution in Scheme 3.

Fig. 11, where the legend of the pressure contour is also used in Figs. 12, 13, 14, 15, 16, 17 and 18.

Scheme 2: Radiator in front of the fuel tank, shown in Fig. 12.

Scheme 3: Radiator in front of the heat exchanger, shown in Fig. 13.

Scheme 4: Radiator between two rear wheels, shown in Fig. 14.

Scheme 5: Radiator on spare tire slot, shown in Fig. 15.

Scheme 6: Radiator at the end of the chassis, shown in Fig. 16.

Scheme 7: Radiator in front of the rear wheels, shown in Fig. 17.

Scheme 8: Radiator behind the rear wheels, shown in Fig. 18.

Schemes Analysis

The important parameters calculated in every scheme are listed in Table II. The projection area of

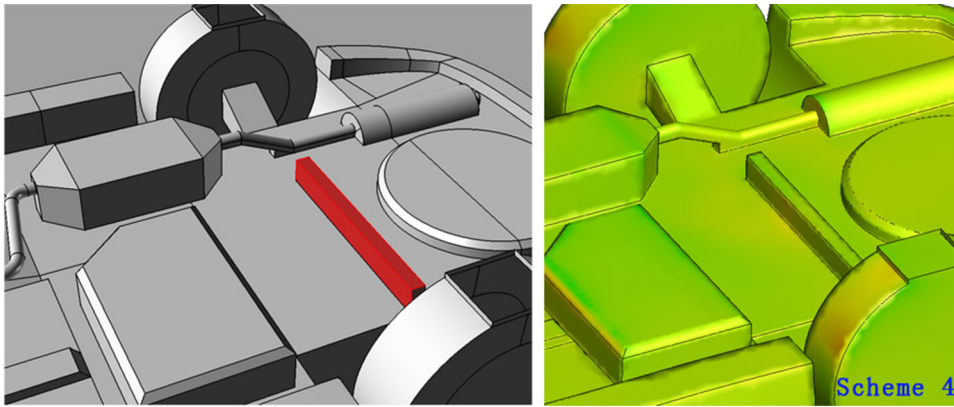


Fig. 14. Model and pressure distribution in Scheme 4.

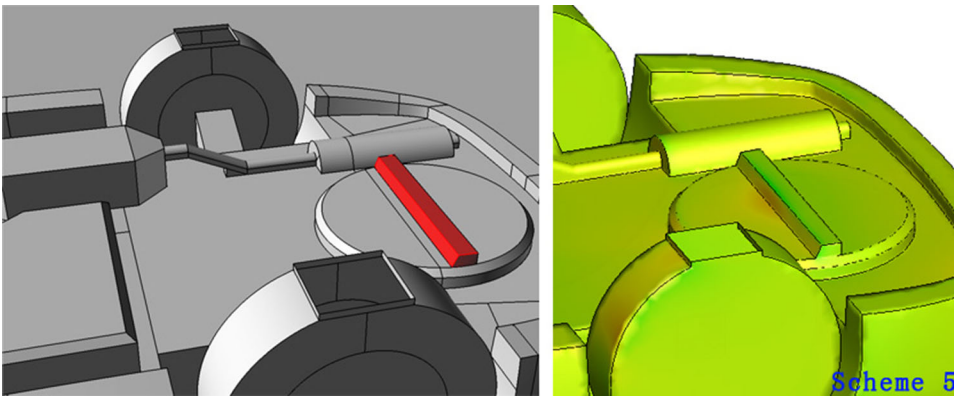


Fig. 15. Model and pressure distribution in Scheme 5.

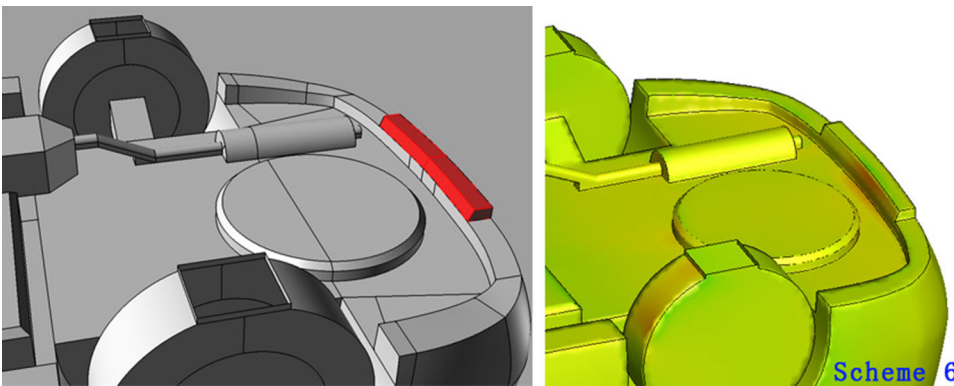


Fig. 16. Model and pressure distribution in Scheme 6.

the TEG and average flow pressure on the radiator surface in flow direction are important to the radiator's cooling performance, which are represented by radiator area and radiator pressure, respectively. The aerodynamic drag coefficient, which is crucial for the car fuel efficiency, is denoted as C_D . A is the projection area of the car in the flow direction. In addition, as the radiator may increase the projection area of the car, the value of $C_D \cdot A$ is added to evaluate the drag force. It is

noted as positive and negative values of $C_D \cdot A$ mean increase and decrease of drag force, respectively.

As the schemes 3, 4, and 5 are illustrated, a TEG radiator acting as a spoiler can reduce the aerodynamic drag force and obtain certain flow pressure for the improvement of cooling performance, which is demonstrated by Table II as well. Therefore, in a practical situation, a reasonable optimization design of the radiator is urgently needed to decrease

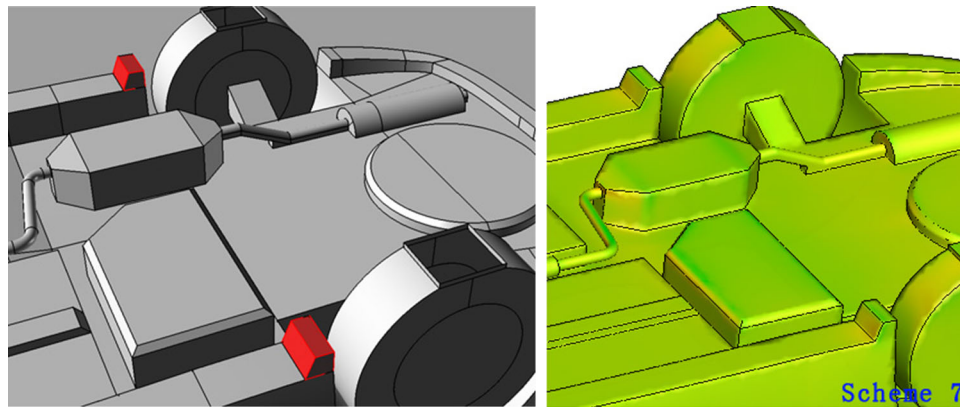


Fig. 17. Model and pressure distribution in Scheme 7.

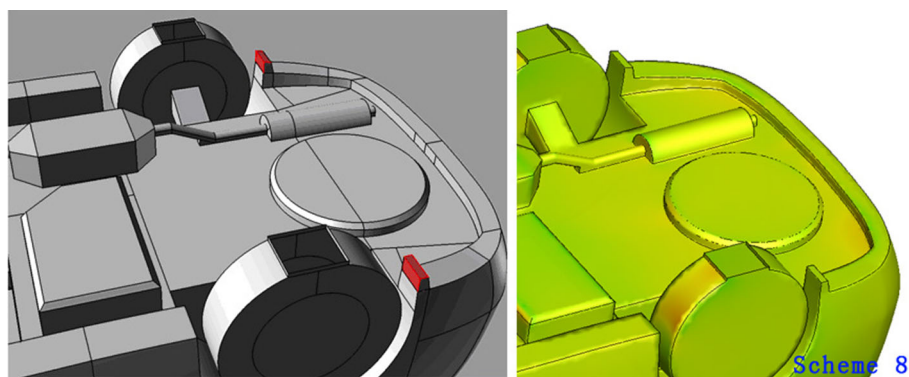


Fig. 18. Model and pressure distribution in Scheme 8.

Table II. Radiator schemes result

	Radiator area (cm ²)	Radiator pressure (Pa)	C _D	A (m ²)	C _D *A (m ²)	C _D *A change
Base model	/	/	0.3074	2.223	0.6834	/
Scheme 1	335	153	0.3138	2.237	0.7019	+2.7%
Scheme 2	270	116	0.3082	2.223	0.6851	+0.3%
Scheme 3	270	104	0.3067	2.223	0.6818	-0.2%
Scheme 4	320	30	0.3065	2.223	0.6813	-0.3%
Scheme 5	245	139	0.3061	2.223	0.6805	-0.4%
Scheme 6	292	190	0.3141	2.223	0.6982	+2.2%
Scheme 7	224	85	0.3092	2.223	0.6874	+0.6%
Scheme 8	144	86	0.3082	2.223	0.6851	+0.3%

the drag force and obtain the higher flow pressure for the enhancement of cooling performance as well.

Because of the departure angle in a car body design, the radiators in most schemes do not influence the value A except in scheme 1, in which a larger radiator causes the increase of the projection area. Hence, except for the drag coefficient C_D, the projection area A should be considered simultaneously.

The TEG radiator is connected to the cooling units by flexible water pipes, thus the position of the radiator is not restricted by the exhaust duct. Therefore, it is possible to optimize the design and

position of the radiator according to different chassis structures, as shown in Fig. 19.

CONCLUSIONS

This paper focuses on the research integration of an exhaust TEG and flow field of a car chassis. Concentrating on the drag force, the projection area, and flow pressure around the radiator, a simulation with a sedan model is conducted by the CFD method. The conclusions are as follows:

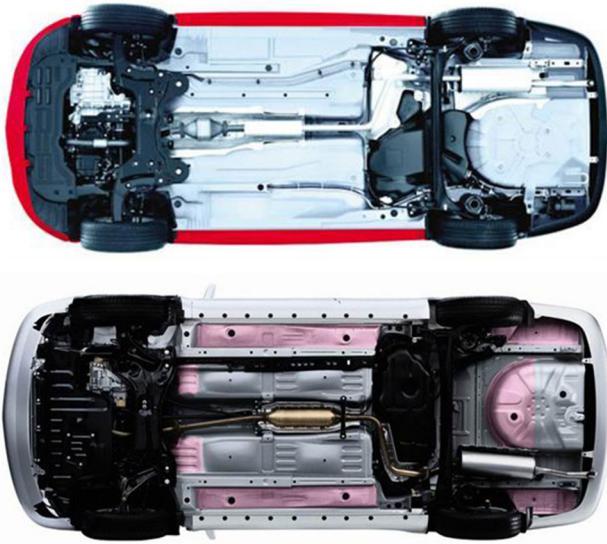


Fig. 19. Radiator design according to chassis structures.

1. The air flow below the car chassis can be used as a cooling source to cool the TEG radiator. What is more, a good radiator configuration can improve the cooling performance, thus providing a better support for the TEG system.
2. The TEG radiator can act as a spoiler to reduce the aerodynamic drag force, hence, reducing the fuel consumption.
3. When designing the configuration of the radiator, both the drag coefficient and projection area of the car should be considered. In addition, a feasible radiator configuration can be realized according to the specific chassis structure.

ACKNOWLEDGEMENTS

This work was funded by Grant No. 2013CB632505 from the National Basic Research Program of China (973 Program) and supported by the Fundamental Research Funds for the Central Universities (WUT142207005).

FUNDING

Grant No. 2013CB632505 from the National Basic Research Program of China (973 Program).

REFERENCES

1. M.A. Karri, E.F. Thacher, and B.T. Helenbrook, *Energy Convers. Manag.* 52, 1596 (2011).
2. F. Frobenius, G. Gaiser, U. Rusche, and B. Weller, *J. Electron. Mater.* 45, 1433 (2016).
3. K.M. Saqr, M.K. Mansour, and M.N. Musa, *Int. J. Automot. Technol.* 9, 155 (2007).
4. S. Kumar, S.D. Heister, X.F. Xu, J.R. Salvador, and G.P. Meisner, *J. Electron. Mater.* 42, 944 (2013).
5. F.P. Brito, A. Alves, J.M. Pires, L.B. Martins, J. Martins, J. Oliveira, J. Teixeira, L.M. Goncalves, and M.J. Hall, *J. Electron. Mater.* 45, 1846 (2016).
6. C.Q. Su, C. Huang, Y.D. Deng, Y.P. Wang, P.Q. Chu, and S.J. Zheng, *J. Electron. Mater.* 45, 1464 (2016).
7. J.W. Qiang, C.G. Yu, Y.D. Deng, C.Q. Su, Y.P. Wang, and X.H. Yuan, *J. Electron. Mater.* 45, 1679 (2016).
8. Y.D. Deng, X. Liu, S. Chen, H.B. Xing, and C.Q. Su, *J. Electron. Mater.* 43, 1815 (2014).
9. W. Mayer and K. Sebastian, *ATZextra Worldw.* 15, 74 (2010).
10. K.S. Song, S.O. Kang, S.O. Jun, H.I. Park, J.D. Kee, K.H. Kim, and D.H. Lee, *Int. J. Automot. Technol.* 13, 905 (2012).
11. Y.P. Wang, S. Li, Y.F. Zhang, X. Yang, Y.D. Deng, and C.Q. Su, *Energy Convers. Manag.* 126, 266 (2016).
12. A. Raveendran, S.N. Sridhara, D. Rakesh, and S.R. Shankapal, *SAE International*, 2009-28-0060 (2009).